Photodecomposition of Iodinated Contrast Media and Subsequent Formation of Toxic Iodinated Moieties during Final Disinfection with Chlorinated Oxidants

Sébastien Allard[a,], Justine Criquet[b], Anaïs Prunier[a], Cécilia Falantin[a,b], Annaïg Le Person[b], Janet Yat-Man Tang[c] and Jean-Philippe Croué[a]*

[a] Curtin Water Quality Research Centre, Department of Chemistry, Curtin University, GPO Box U1987, Perth WA 6845, Australia

[b] Université Lille 1 Sciences and Technologies, LASIR, UMR CNRS 8516, 59655 Villeneuve d'Ascq, France

[c] National Research Centre for Environmental Toxicology (Entox), The University of Queensland, Brisbane QLD 4108, Australia

*Corresponding author phone: +61 8 9266 7949; email: s.allard@curtin.edu.au

Abstract

Large amount of iodinated contrast media (ICM) are found in natural waters (up to μg/L levels) due to their worldwide use in medical imaging and their poor removal by conventional wastewater treatment. Synthetic water samples containing different ICM and natural organic matter (NOM) extracts were subjected to UV_{254} irradiation followed by the addition of chlorine (HOCl) or chloramine (NH_2Cl) to simulate final disinfection. In this study, two new quantum yields were determined for diatrizoic acid (0.071 mol.Einstein^{-1}) and iotalamic acid (0.038 mol.Einstein^{-1}) while values for iopromide (IOP) (0.039 mol.Einstein^{-1}), iopamidol (0.034 mol.Einstein^{-1}) and iohexol (0.041 mol.Einstein^{-1}) were consistent with published data. The photodegradation of IOP led to an increasing release of iodide with increasing UV doses. Iodide is oxidized to hypoiodous acid (HOI) either by HOCl or NH_2Cl. In presence of NOM, the addition of oxidant increased the formation of iodinated disinfection by-products (I-DBPs). On one hand, when the concentration of HOCl was increased, the formation of I-DBPs decreased since HOI was converted to iodate. On the other hand, when NH_2Cl was used the formation of I-DBPs was constant for all concentration since HOI reacted only with NOM to form I-DBPs. Increasing the NOM concentration has two effects, it decreased the photodegradation of IOP by screening effect but it increased the number of reactive sites available for reaction with HOI. For experiments carried out with HOCl, increasing the NOM concentration led to a lower formation of I-DBPs since less IOP are photodegraded and iodate are formed. For NH_2Cl the lower photodegradation of IOP is compensated by the higher amount of NOM reactive sites, therefore, I-DBPs concentrations were constant for all NOM concentrations. 7 different NOM extracts were tested and almost no differences in IOP degradation and I-DBPs formation was observed. Similar behaviour was observed for the 5 ICM tested. Both oxidant poorly degraded the ICM and a higher formation of I-DBPs was observed for the chloramination experiments compared to the chlorination experiment. Results from toxicity testing showed that the photodegradation products of IOP are toxic and confirmed that the formation of I-DBPs leads to higher toxicity. Therefore, for the experiment with HOCl where iodate are formed the toxicity was lower than for the experiments with NH_2Cl where a high formation of I-DBPs was observed.

Keywords: iodinated disinfection by-products (I-DBPs), UV, toxicity, iodinated X-ray contrast media, natural organic matter, quantum yield.

53 # 1. Introduction

54 X-ray contrast media are a class of pharmaceuticals used for the imaging of internal organs, blood
55 vessels and soft tissues during radiological and medical diagnostic procedures (Pérez and Barceló,
56 2007). Currently, iodinated contrast media (ICM) are the most widely administered intravascular
57 pharmaceuticals with doses up to 120 g in radiographic procedures (Busetti et al., 2010, Christiansen
58 2005). The worldwide consumption of ICM is approximately 3.5×10^6 kg/year (Pérez and Barceló,
59 2007). In contrast to most pharmaceuticals, ICM are not designed to have a specific therapeutic
60 activity. These compounds are metabolically stable and are almost completely excreted from the
61 body via urine or faeces within a day of administration (Pérez and Barceló, 2007, Ternes and Hirsch,
62 2000). Therefore, they are transferred to the wastewater. Several studies have shown that the high
63 concentration of adsorbable organic iodine (AOI) in hospital and clinical wastewaters can be
64 explained by the presence of ICM (Drewes et al., 2001, Putschew et al., 2001, Gartiser et al., 1996).
65 Since ICM are highly soluble and poorly biodegradable they are not significantly removed by
66 conventional wastewater treatments. Hence ICM are found at high concentrations (μg/L levels)
67 downstream in rivers and groundwaters (Pérez and Barceló, 2007, Ternes and Hirsch, 2000,
68 Putschew et al., 2000, Wendel et al., 2014)). Even though ICM are not toxic as such, they recently
69 received attention since appreciable concentrations of genotoxic/cytotoxic iodinated disinfection by-
70 products (I-DBPs) were detected in drinking waters containing very low or no detectable natural
71 iodine levels (Richardson et al., 2008). It was demonstrated that ICM, which participate to the pool of
72 iodine in the environment, may be degraded during drinking water treatment and may promote the
73 formation of I-DBPs (Duirk et al., 2011).

74 Recently, several studies focused on the impact of various oxidative treatment such as chlorine
75 (HOCl), monochloramine (NH_2Cl) or chlorine dioxide on ICM degradation (Wendel et al., 2014, Duirk
76 et al., 2011, Ye et al., 2014). These disinfectants are not able to oxidise ICM with the exception of
77 iopamidol, which is oxidized by HOCl (0.87 M s^{-1} at pH 8.5) (Wendel et al., 2014) and leads to a
78 significant formation of iodinated trihalomethanes (I-THMs) in presence of natural organic matter
79 (NOM) (Duirk et al., 2011, Ye et al., 2014). Duirk et al., (2011) demonstrated that the presence of
80 iopamidol in source waters (presence of NOM) did not induce toxicity. However, after chlorination
81 the genotoxicity of the waters was enhanced (LC_{50} = 117.5 μM). Wendel et al., (2014) showed some
82 toxicity related to the chlorination of iopamidol in ultra-pure water (without NOM) but to a lower
83 level (LC_{50} = 427 μM). Five high-molecular weight iopamidol chlorination DBPs were isolated and it
84 was shown that they were minor contributors to the overall cytotoxicity and genotoxicity (Wendel et
85 al., 2016). Photolysis by sunlight (Pérez et al., 2009, Doll and Frimmel, 2003) or low/medium pressure
86 mercury lamp (Canonica et al., 2008, Pereira et al., 2007a, Pereira et al., 2007b) was found to be

87 efficient in degrading ICM. Under simulated solar radiation, photolysis of ICM leads to a gradual
88 deiodination of the aromatic ring, *i.e.* iodide (I^-) is released in solution (Pérez et al., 2009, Doll and
89 Frimmel, 2003). The same behaviour was observed under low pressure UV lamp for iopamidol (Tian
90 et al., 2014).

91 When iodide-containing waters are disinfected by HOCl or NH_2Cl, I^- is oxidized to hypoiodous acid
92 (HOI). In presence of HOCl, HOI can be further oxidized to iodate (IO_3^-) or can react with NOM to form
93 I-DBPs (Bichsel and von Gunten, 1999, Criquet et al., 2012). The formation of IO_3^- is not a toxicological
94 concern because it is quickly reduced *in vivo* to I^- (Burgi et al., 2001) and is therefore the desired sink
95 for iodine during water treatment. When NH_2Cl is used as oxidant, the formation of IO_3^- is extremely
96 slow, thus HOI is stable in solution and reacts with NOM to form I-DBPs (Jones et al., 2011, Hua and
97 Reckhow, 2007a, Kristiana et al., 2009, Bichsel and von Gunten, 2000a). I-DBPs are not regulated,
98 even though, it is generally admitted that they are more toxic than their chlorinated and brominated
99 DBPs analogues (Richardson et al., 2008, Plewa et al., 2004, Plewa et al., 2008). For example, the
100 iodoacetic acid has been identified as the most cytotoxic and genotoxic DBP identified to date
101 (Richardson et al., 2008, Plewa et al., 2004).

102 UV disinfection of drinking water is commonly implemented in Europe and generally consists of a low
103 pressure mercury lamp emitting at 254 nm. UV has been used since it is efficient in inactivating a
104 wide range of waterborne pathogens while it does not produce regulated DBPs (Wolfe 1990). It leads
105 to a lower oxidant demand and therefore, the amount of chlorinated oxidant needed to ensure a
106 disinfectant residual in the distribution system is reduced as well as the subsequent formation of
107 regulated DBPs. It has been shown in a previous study, carried out in ultrapure water (absence of
108 NOM), that the combination of UV photolysis with post-disinfection applied on a iopamidol solution
109 enhanced the formation of I-DBPs (Tian et al., 2014). Therefore, in real system where NOM is present
110 the formation of I-DBPs is expected to be even higher and this sequential process might not be
111 beneficial in presence of ICM.
112 In a first stage the kinetics and direct phototransformation quantum yields of 5 ICM (iopromide (IOP),
113 iopamidol, diatrizoic acid, iohexol and iotalamic acid) under low-pressure lamp irradiation were
114 determined. In a second stage the degradation of ICM and the formation of I-DBPs from the
115 combination of UV followed by chlorination or chloramination in synthetic waters with and without
116 NOM were investigated. To better understand the main factors affecting the formation of potentially
117 toxic I-DBPs from the sequential oxidation process, the influence of the UV fluence, concentration of
118 oxidants, NOM type and concentration were investigated using IOP. Finally, *in vitro* cell-based toxicity
119 testing was carried out for specific experimental conditions.

120

2. Materials and methods

2.1. Chemicals and reagents

All chemicals and solvents were of the highest analytical grade and used without further purification. The ultrapure water was produced using an IBIS Technology Ion Exchange System followed by Elga Purelab Ultra System (TOC <0.2 mgC L^{-1} and 18.2 mΩ cm) . Disposable syringe filters (Acrodisc®, 0.45 µm pore size, 25 mm diameter) were purchased from PALL Life Sciences (NY, USA). Suwannee River (SR), Nordic Reservoir (NR) and Pony Lake fulvic acid (PL) NOM were purchased from the International Humic Substance Society (IHSS, USA), while other NOM extracts were previously isolated according to a protocol detailed elsewhere (Leenheer and Croue, 2003) (Table S1). All ICM were reference standard grade and were purchased from United States Pharmacopeia–USP, Maryland, USA. The chemical structures of the 5 ICM selected for this study are shown in Table 1.

Table 1: Structure and chemical properties of ICM

Amidotrizoic acid (Diatrizoic acid) *3,5-diacetamido-2,4,6-triiodobenzoic acid* $C_{11}H_9I_3N_2O_4$ - M_W =613.91 g.mol^{-1}	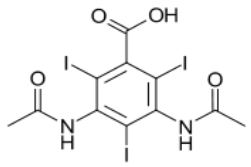
Iohexol *1-N,3-N-bis(2,3-dihydroxypropyl)-5-[N-(2,3 dihydroxypropyl)acetamido]-2,4,6-triiodobenzene-1,3-dicarboxamide* $C_{19}H_{26}I_3N_3O_9$ - M_W =821.14 g.mol^{-1}	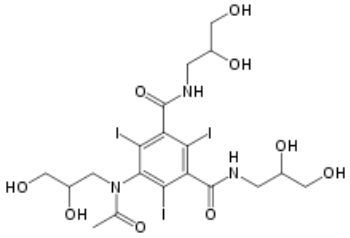
Iopamidol *1-N,3-N-bis(1,3-dihydroxypropan-2-yl)-5-[(2S)-2-hydroxypropanamido]-2,4,6-triiodobenzene-1,3-dicarboxamide* $C_{17}H_{22}I_3N_3O_8$ - M_W =777.09 g.mol^{-1}	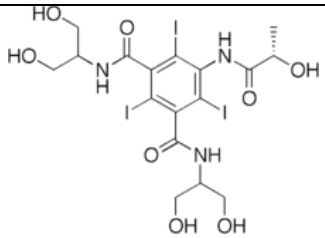
Iopromide *(1-N,3-N-bis(2,3-dihydroxypropyl)-2,4,6-triiodo-5-(2-methoxyacetamido)-1-N-methylbenzene-1,3-dicarboxamide* $C_{18}H_{24}I_3N_3O_8$ - M_W =791.11 g.mol^{-1}	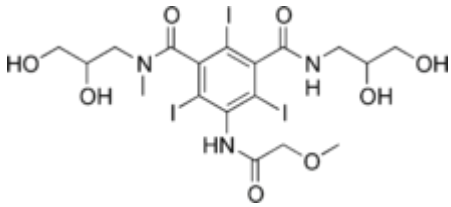
Iotalamic acid *3-acetamido-2,4,6-triiodo-5-(methylcarbamoyl)benzoic acid* $C_{11}H_9I_3N_2O_4$- M_W =613.91 g.mol^{-1}	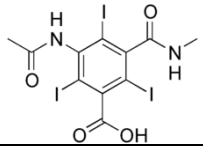

133 **2.2. Experimental set up**

134 The reactor vessel was equipped with a 15 W low-pressure mercury (LP Hg) lamp (Heraeus
135 Noblelight, model TNN 15/32) emitting monochromatic UV light at 254 nm. The lamp was introduced
136 in the axial position into a 1.5 L cylindrical reactor and was kept separated from the aqueous solution
137 by a quartz glass and a cooling jacket using recirculating water at 20°C (Figure S1). The optical width
138 was 2.8 cm. The aqueous solutions were stirred with a magnetic bar throughout the entire time of
139 the experiments in order to maintain a homogeneous solution. The incident photonic flux received
140 by the solutions was determined by chemical actinometry using hydrogen peroxide (Nicole et al.,
141 1990) and/or atrazine actinometry (Canonica, et al., 1995). An actinometry was carried out for each
142 set of experiments.

143 **2.3. Analytical methods**

144 ICM were analysed using an Agilent 1100 HPLC system equipped with a diode array absorbance
145 detector. The column was an Alltima C18 (4.6*250 mm, 5 µm particle size). The mobile phase
146 consisted of 10% methanol and 90% ultrapure water (acidified with 0.2% of acetic acid) at a flow rate
147 of 1 mL min^{-1}. I^- and IO_3^- were measured simultaneously via ion-chromatography (IC) using a Dionex
148 ICS3000 according to the method of Salhi and von Gunten (1999). The limits of detection (LOD) were
149 5 $\mu g.L^{-1}$ for I^- and 1 $\mu g.L^{-1}$ for IO_3^-.

150 AOI was analysed according to the following procedure. Samples were acidified to pH 2 and enriched
151 by adsorption onto a granular activated carbon column (GAC 0.4 µg/40 mg CPI International USA)
152 using a Mitsubishi TOX sampler preparator. Inorganic halides were washed out with a nitrate
153 solution. Then the GAC was placed in a quartz sample boat, introduced into the combustion chamber
154 (Mitsubishi AQF-100 Automatic Quick Furnace) and heated at high temperature (1000°C) during 10
155 minutes under a flow of nitrogen. During the combustion process the AOI was reduced to I^- and
156 volatilised, before being trapped in ultrapure water and injected to the IC. Chromatographic analysis
157 was carried out with a AS11 column (Dionex) and a mobile phase constituted of a 25 mM KOH at a
158 flow rate of 1 $mL.min^{-1}$.

159 Chlorinated and iodinated THMs were analysed by headspace solid-phase microextraction-gas
160 chromatography mass spectrometry according to a previously published method (Allard et al., 2012).

161 **2.4. Experimental procedure**

162 *Kinetics and quantum yield determination.* Working solutions containing individual ICM at 10 µM
163 were freshly prepared in ultrapure water for each analytical run. For each experiment, the pH was
164 controlled with a 5 mM phosphate buffer adjusted with NaOH and/or HCl. 500 mL of ICM solutions

were irradiated for up to five minutes and samples were collected every 10 seconds. Similar IOP degradation was observed in both static (kinetic experiment) and UV dose experiments (Figure S2). This shows that for the static irradiation experiments, the volume loss induced by the withdrawing of the samples did not affect the overall degradation of ICM, i.e. the incident photonic flux received by the solution is constant.

ICM degradation and formation of I-DBPs. Since it is one of the most commonly used ICM, IOP was selected to develop a detailed mechanistic study on the formation of potentially toxic iodinated organic compounds. The desired volume of a concentrated NOM solution was added to the solution in order to reach the target concentrations of 2 and 4 mgC/L. The influence of NOM nature was also tested using NOM isolates described in Table S1. The irradiation dose was calculated using the incident photonic flux determined by actinometry and ranged from 400 to 50000 $J.m^{-2}$. After irradiation, the chlorinated oxidant (1, 2 and 5 $mgCl_2/L$) was injected to the solution. The mixture was left at room temperature for 24 h, to simulate a typical residence time in distribution systems and to allow sufficient contact time between the oxidants and the irradiated solution containing NOM and ICM to form I-DBPs. After 24 h, the oxidant concentration remaining in the solution was determined by the *N,*N-diethyl-p-phenylenediamine (DPD) method (APHA 1998), if a residual oxidant concentration was observed, the samples were quenched by adding a slight excess (5%) of ascorbic acid.

To compare the reactivity of the different ICM and their potential to form I-DBPs through sequential UV, chlorination/chloramination treatment, working solutions containing individual ICM at 10 µM and 2 mgC/L of Suwannee River NOM were prepared. The solutions were irradiated at 4000 $J.m^{-2}$ followed by the addition of 5 $mgCl_2/L$ of oxidant (HOCl or NH_2Cl). For each experiment, the concentrations of ICM, I^-, IO_3^-, THMs and AOI were determined with the analytical methods described above.
All experiments were carried out at least in duplicate.

Cell-based in vitro toxicity testing. Reactive toxicity was assessed with the AREc32 bioassay for oxidative stress response according to the protocol described in (Escher et al., 2013). For this purpose, 500 mL of solution was irradiated and eventually chlorinated or chloraminated in the same conditions as previously presented. A preconcentration step was performed on SPE cartridges (Tang et al., 2013). The extracts were tested in duplicate on both bioassays and the results were presented in relative enrichment factor (REF). REF is a measure of how much a sample is enriched/concentrated. Bioanalytical equivalent concentrations were determined with the reference compound of each bioassay, *i.e.*, tert-Butylhydroquinone (tBHQ) was used in the AREc32 bioassay to determine the tBHQ-equivalent concentration (tBHQ-EQ) (Escher et al., 2013).

199 # 3. Results and discussion

200 ## 3.1 Determination of direct phototransformation rates and quantum yields at 254 nm

201 UV absorption spectra of the 5 ICM were recorded at pH 4, 7 and 10. All spectra are presented in
202 Figure S3 and confirmed that pH did not affect their absorption properties at 254 nm.

203 Molar extinction coefficient values at 254 nm (ε_{254}) were determined for the 5 ICM (Table 2).

204 **Table 2: Molar extinction coefficient and quantum yields of ICM at 254 nm and pH 7.**

Compounds	ε_{254} (10^3) ($M^{-1}.cm^{-1}$)	Φ_{254} (10^{-2}) (mol/Einstein)
Iopromide	22.1 (± 0.48) / 21.0*[1]	3.9 (± 0. 2) / 3.9*[1]
Iohexol	27.7 (± 0. 08) / 27.6*[2]	4.1 (± 0.3) / 4.0*[2]
Iopamidol	22.0 (± 0. 17) / 22.7*[3]	3.4 (± 0.1) / 3.3*[3]
Iotalamic acid	19.1 (± 0. 21)	3.8 (± 0.3)
Diatrizoic acid	15.9 (± 0. 07)	7.1 (± 0.3)

205 **** Molar extinction coefficients already reported in the literature [1](Canonica et al., 2008), [2](Wols and Hofman-Caris 2012)***
206 ***and [3](Tian et al., 2014).***

207 ε_{254} determined in this study for IOP, iohexol and iopamidol are consistent with the values previously
208 reported in literature (Table 2). Additionally, ε_{254} for iotalamic acid and diatrizoic acid were
209 determined to be 19100 and 15900 $M^{-1}.cm^{-1}$, respectively. All ε_{254} values were found to be in the
210 same range since the 5 ICM have similar structure.

211 For the determination of the quantum yields, irradiation experiments were carried out at an incident
212 photonic flux ranging from 3.93 to 4.43 µEinstein.s^{-1} (14 repetitions). The degradation of the 5 ICM
213 under UV irradiation as a function of time and UV dose is presented in Figure S4. After 120 seconds
214 of UV exposure (14000 J m^{-2}), almost all ICM were fully decomposed. This finding confirms that UV
215 treatment is efficient in degrading ICM. The UV degradation of the 5 ICM follows a first order kinetic
216 law allowing to calculate the first order photolysis rate constant k_{obs} using the slope of equation (1):

217 $$Ln(10^{D}-1) = Ln(10^{Do}-1) - k_{obs}\, t \qquad (1)$$

218 With D: Absorbance of the solution and D_0: Absorbance of the initial solution ($D = \varepsilon_{254}\, l\, C$; with l:
219 optical path and C: concentration). The absorbances are calculated from the concentrations of ICM
220 determined by HPLC and the molar extinction coefficient determined previously. Examples of curve
221 linearization are presented in Figures S5.

222 The quantum yield was calculated using the molar extinction coefficient determined previously, the
223 apparent incident photonic flux and the photolysis rate constant of each ICM, according to equation
224 (2):

225 $\phi = k_{obs} V / 2{,}3 \varepsilon l I_o S_\lambda$ (2)

226 with ϕ: quantum yield (mol.Einstein^{-1});
227 k_{obs}: pseudo first order photolysis rate constant (s^{-1});
228 V: volume of the reactor (L);
229 ε: molar extinction coefficient ($M^{-1}.cm^{-1}$)
230 l: optical path (cm)
231 I_0 : incident photonic flux (Einstein.s^{-1}) and
232 S_λ: Morowitz correction factor
233
234 The incident photonic flux determined by actinometry with both hydrogen peroxide and atrazine is
235 valid for a solution that has a negligible absorbance (< 0.02). In this study, the absorbance of ICM in
236 ultrapure water was larger than 0.02, since we used a higher concentration for a better analytical
237 resolution in HPLC. Therefore, a correction factor, the Morowitz correction factor (S_λ), should be
238 introduced in the fluence calculation (Katsoyiannis et al., 2011). To determine the quantum yield, the
239 incident photonic flux was multiplied by the Morowitz factor specific to each ICM. Table S2
240 summarizes the correction factors for each ICM. Details of calculation for the correction factors are
241 found in Text S1. The quantum yields determined for IOP (0.039 mol.Einstein^{-1}), iopamidol (0.034
242 mol.Einstein^{-1}) and iohexol (0.041 mol.Einstein^{-1}), are consistent with the values reported in the
243 literature (Table 2). This confirms that the experimental set up and calculation were accurate. Two
244 new quantum yields were determined in this study; diatrizoic acid (0.071 mol.Einstein^{-1}) and
245 iotalamic acid (0.038 mol.Einstein^{-1}). The influence of pH on iopamidol and iohexol degradation was
246 studied and found to be negligible (Figure S6). It was assumed that the other ICM behave similarly.
247 This allows to evaluate the extent of these ICM degradation during UV disinfection since the kinetic
248 rate constants and quantum yields are not pH dependent (in the pH range found in water treatment).

249 **3.2 Degradation of iopromide under low pressure UV_{254} irradiation**

250 Preliminary experiments were carried out in absence of NOM. The degradation of IOP (10 µM) at
251 various UV doses (400, 1000, 2000, 4000, 6000 and 10000 J.m^{-2}) and pH 7 as well as the evolution of
252 the different iodine species formed after UV_{254} irradiation are presented in Figure 1. I^-, IO_3^-, IOP and
253 AOI concentrations were measured to understand the main mechanisms involved during UV
254 disinfection. AOI measurements include the remaining IOP, the products formed from photolysis

which still contain iodine in their structures, and the eventual subsequent by-products formed by reaction of reactive iodine species with organic moieties. It has been shown that the photolysis of iodide could lead to the formation of iodine radical and/or iodine reactive species (Jortner et al., 1961, Sauer Jr et al., 2004); therefore, these species could react with organics moieties to form I-DBPs. In the following of the manuscript, HOI will be used to represent all the iodine reactive species which also includes IO^- and I_2. HOI was reduced to I^- during quenching, therefore, the measured I^- stands for the sum of HOI and I^-. The concentration of the different iodine species are normalised to the total iodine content since IOP contains several iodine atoms. IOP is presented as [IOP]/[IOP]$_o$ (since [IOP]$_o$ = [IOP]$_{max}$) while for other iodinated species, for example for I^-, it is presented as [I^-]/[I^-]$_{max}$, with [I^-]$_{max}$ = 3 × [IOP]$_0$ to compare the evolution of the different species.

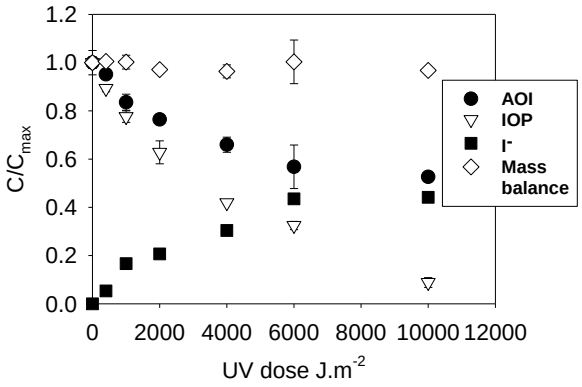

Figure 1: Degradation of iopromide under low pressure UV irradiation and evolution of iodine species expressed in iodine equivalent. [IOP]$_o$ 10 µM; pH 7; 5 mM phosphate buffer. The concentration of iodate was under the limit of detection.

As shown in Figure 1, the IOP concentration decreased with increasing UV doses (exposure time multiplied by photon incident photonic flux of the lamp) with less than 1 µM remaining in solution (~90% degradation) for a dose of 10000 J.m^{-2}. Conversely, the I^- concentration increased up to 14 µM (corresponding to 45% of the initial iodine content in iopromide) and was equal to total iodine minus AOI concentration and decreased from 30 to 16 µM (corresponding to 55% of the initial iodine content) for a dose of 10000 J.m^{-2}. The mass balance (sum of I^- and AOI) is consistent for the different UV doses. This confirms the findings of Doll and Frimmel (2003) and Perez et al., (2009) obtained under simulated solar light with IOP and results for iopamidol obtained under low pressure UV lamp irradiation (Tian et al., 2014)) which observed the release of I^- in solution. It was also verified that the UV degradation of IOP does not lead to the formation of IO_3^- and/or HOI (the absence of HOI was verified by spiking an excess of phenol to form iodophenol that can be detected by high pressure liquid chromatography (Allard et al., 2009)). It can be assumed that the concentration of reactive iodine (HOI or I_2) is low in our experimental conditions. Thus, the determined AOI only corresponds

282 to the remaining IOP and its photodegradation products; no additional by-products are formed
283 during the photolysis.

284

285 **3.3 Effect of UV_{254} photolysis followed by chlorination/chloramination on iopromide degradation in**
286 **absence and presence of NOM**

287

288 In drinking-water treatment, German and Austrian regulations prescribe a disinfection dose (fluence)
289 of 400 $J.m^{-2}$ (Canonica et al., 2008). In Australia, a fluence of 2000 $J.m^{-2}$ is used to inactivate
290 adenoviruses. Based on the IOP degradation results a photon incident photonic flux of 4000 $J.m^{-2}$
291 was chosen for further experiments since approximately 50% of IOP is degraded at this treatment
292 dose. The impact of the subsequent addition of HOCl or NH_2Cl has been studied to evaluate the risk
293 of I-DBPs formation and related toxicity during final disinfection in distribution system. Various
294 oxidant concentrations (0, 1, 2 and 5 $mgCl_2/L$ of HOCl or NH_2Cl) were added to the solution after UV
295 irradiation (dose of 4000 $J.m^{-2}$) in absence or presence of NOM and left for 24H.
296 As shown in Figure 2a, in absence of NOM, the addition of HOCl induces a slight decrease of the
297 residual IOP. IOP concentration decreases from 51% of the initial concentration after UV treatment
298 to 45% for 2 $mgCl_2/L$ of HOCl and 33% for 5 $mgCl_2/L$ of HOCl. For the experiments with NH_2Cl, no
299 significant further degradation of IOP was observed.

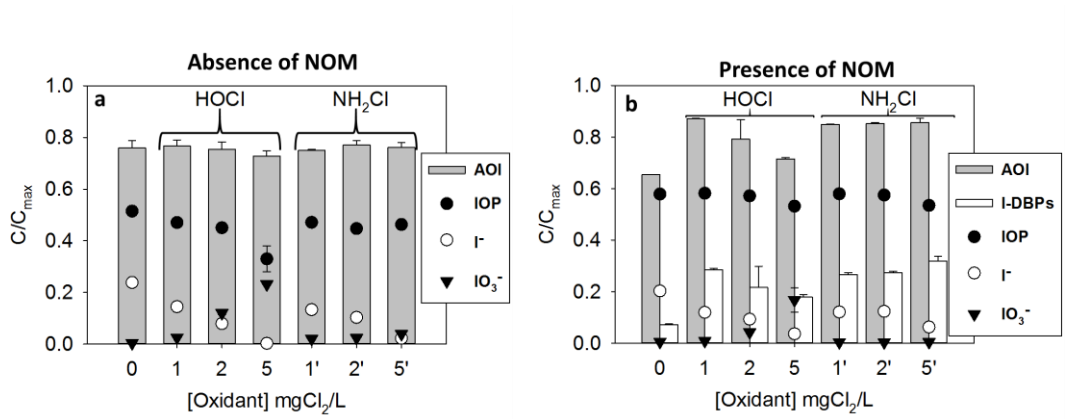

300

301 **Figure 2: Influence of chlorine or chloramine doses (24H contact time) on iopromide degradation**
302 **and on the speciation of iodine after irradiation in presence or absence of DOM. UV dose 4000 $J.m^{-2}$,**
303 **$[IOP]_o$ 10 µM, [HOCl] or [NH_2Cl] 0, 1, 2, 5 $mgCl_2/L$, a) absence of NOM, b) 2 mgC/L SR-NOM.**

304

305 These results are differing from the finding reported in Wendel et al., (2014), which shows no
306 degradation of IOP by HOCl or NH_2Cl. Nevertheless, the photodecomposition is the main degradation
307 pathway accounting for a ~50% reduction of the initial concentration. The concentration of I^- is
308 decreasing from 23% of the initial iodine content to ~0% for increasing oxidant concentration for

both HOCl and NH_2Cl (Figure 2a). For the chlorinated solution, the decrease of iodide concentration is explained by the formation of IO_3^-. I^- is oxidized to HOI by reaction with HOCl, which could further react to produce IO_3^-. For chloraminated solutions, IO_3^- is not/poorly formed due to the inability of NH_2Cl to oxidize I^- further than HOI (Bichsel and von Gunten, 1999). Therefore, it cannot explain the decrease in I^- concentration. HOI can also disproportionate to I^- and IO_3^- (Bichsel and von Gunten, 2000b). However, in our case, even though small concentrations of IO_3^- are measured it does not account for the entire loss of HOI. Since no NOM was added to the solution the only iodinated organic compounds present in solution are IOP, its decomposition products and I-DBPs formed through reaction of HOI with the decomposition products. In the case of NH_2Cl, the I^- concentration should be inversely correlated to the AOI to complete the mass balance. As shown in Figure 2a, the AOI remains constant (within the error bars range) while the iodide concentration decreases in all experiments. Therefore, the concentration of I-DBPs formed from reaction of HOI with IOP decomposition products represents only a small fraction of the AOI and it can be concluded that the decomposition products are poorly reacting with HOI. One can notice that the mass balance (sum of AOI, I^- and IO_3^-), is decreasing with increasing NH_2Cl dose. This may be explained by the loss of HOI through volatilization (Figure S7). It was found that a large portion (~60%) of iodine disappears in 24H when comparing samples containing 30 μM of HOI with and without headspace. Experiments are currently underway in our laboratory to better explain this behaviour.

Similar experiments were carried out in presence of 2 mgC/L SR-NOM. White bars in Figure 2b represent I-DBPs calculated by subtracting the concentration of AOI (grey bars) to the concentration of IOP (black circle) expressed in iodine equivalent (concentration of IOP multiplied by the number of iodine atoms). It represents both iodinated organic compounds formed by reaction between HOI and NOM and the degradation products of IOP that still contains iodine in their structure. Figure 2b shows that for both disinfectants, the degradation of IOP is slightly reduced in presence of NOM (remaining IOP in solution: ~5.7 μM or 57% and ~5.1 μM or 51% in presence and absence of NOM respectively). The addition of the disinfectants after the photolysis step induced almost no degradation of IOP except for the highest oxidant dose (5 $mgCl_2/L$) where a slight degradation is observed. However, it should be noticed that the degradation of IOP by HOCl for 5 $mgCl_2/L$ is much lower in presence of NOM, probably because a substantial part of the HOCl is rapidly consumed by NOM. The addition of NOM is increasing the formation of I-DBPs for both HOCl and NH_2Cl. This is due to the formation of iodinated organic moieties by reaction between HOI and NOM. Since the concentration of IOP degraded is almost constant, the variation of AOI is only due to the formation of I-DBPs from the reaction between HOI and NOM. The concentration of I^- decreases for both disinfectants because I^- released during UV_{254} irradiation is oxidized to HOI and reacts to form I-DBPs and/or IO_3^-.

Figure 2b also shows that when the HOCl dose increases, the concentrations of AOI and I-DBPs decreased. HOI has a higher reactivity towards phenolic structures than HOCl (Lee et al., 2005), however when the HOCl concentration is increased, the competition between HOI and HOCl towards NOM reactive sites increases. Therefore, more reactive sites are used up by HOCl and less reactive sites are available for reaction with HOI and subsequent formation of I-DBPs. Furthermore, the oxidation of HOI to iodate is enhanced for high HOCl concentrations. There was no oxidant residual after 24H for the experiment with 1 and 2 $mgCl_2/L$. For low HOCl concentrations, HOCl was exhausted by reaction with both NOM and I^- and a fraction of iodine was present as HOI and available to react solely with NOM to form I-DBPs. For high HOCl doses where an oxidant residual was present, HOCl was available and reacted with HOI to form IO_3^-. Therefore, when increasing HOCl concentration from 1 to 5 $mgCl_2/L$, I-DBPs concentration decreases from 28% to 18% of the initial iodine content. Conversely, the formation of IO_3^- increases with increasing HOCl doses (to a lower extent compared to the experiment without NOM). For example, for the experiment without NOM 12% and 23% of iodine was converted to IO_3^- after sequential treatment while in presence of NOM only 4% and 17% of iodine was converted to IO_3^- for 2 and 5 $mgCl_2/L$, respectively (this is also due to the lower IOP degradation and the resulting lower concentration of I^- released). For the experiments with NH_2Cl, the AOI (85%) and I-DBPs (~27%) concentrations remain constant (a slight increase in I-DBPs and decrease in concentration of IOP is observed for 5 $mgCl_2/L$). Since an oxidant residual from 0.3 to 2.0 $mgCl_2/L$ was measured after 24H for 1 to 5 $mgCl_2/L$, respectively, I^- is continuously oxidised to HOI (no IO_3^- are formed) that leads to similar I-DBPs formation. It can be noticed that there is still I^- present in solution even for 5 $mgCl_2/L$ HOCl. This suggests that HOI was in excess compared to the amount of NOM's reactive sites. Under these conditions, several I-THMs could be formed by halogen substitution (i.e., I or Cl). The formation of chlorinated and iodinated THMs is presented in Figure 3.

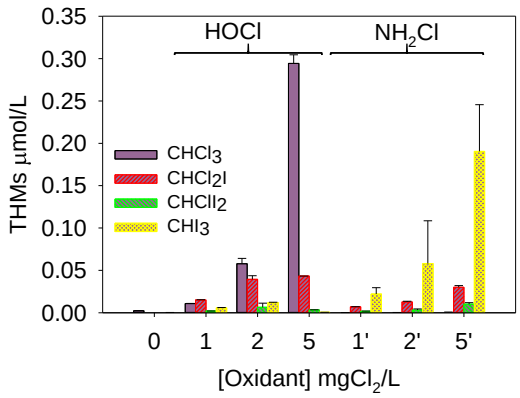

Figure 3: THMs formation in presence of NOM after irradiation of iopromide followed by chlorination or chloramination at various doses. UV dose 4000 $J.m^{-2}$, $[IOP]_o$ 10 µM, [HOCl] or $[NH_2Cl]$ 0, 1, 2, 5 $mgCl_2/L$ (24H contact time), 2 mgC/L SR-NOM.

371 Figure 3 shows that during chlorination dichloroiodomethane ($CHCl_2I$) and chloroform ($CHCl_3$) are the
372 main THMs formed (Allard et al., 2015). As expected $CHCl_3$ increases and only small concentrations of
373 I-THMs were detected with increasing HOCl doses due to the oxidation of I^- to IO_3^- and the high
374 chlorination of NOM reactive sites. Increasing the HOCl dose shift the speciation of the THMs from
375 $CHCl_2I$ to $CHCl_3$ because HOCl and iodine are competing for incorporation to the trihalomethanes
376 (Bichsel and von Gunten, 2000a). Although, since iodine become minor compared to chlorine when
377 high concentrations of oxidant are present, the formation of IO_3^- is favored. When NH_2Cl is used as
378 disinfectant, iodoform (CHI_3) is the main THM formed and its concentration increases with NH_2Cl
379 concentration as reported in previous studies (Duirk et al., 2011, Ye et al., 2014, Bichsel and von
380 Gunten, 2000a). Since NH_2Cl is a poor halogenating agent, HOI is not competing for NOM reactive
381 sites. Furthermore, HOI persists longer in solution because the oxidation of HOI to IO_3^- is extremely
382 slow, and has more opportunities to react with the organic matrix (Ye et al., 2014). It is interesting to
383 note that the formation of I-THMs is not correlated to the total formation of I-DBPs. For HOCl the I-
384 DBPs concentration clearly decreases from 1 $mgCl_2/L$ to 5 $mgCl_2/L$ (Figure 2b) while the iodine
385 incorporation into THMs increases from 1 to 2 $mgCl_2/L$ and then decreases for 5 $mgCl_2/L$ (Figure 3).
386 For NH_2Cl, CHI_3 concentration increases continuously with increasing NH_2Cl concentration (Figure 3)
387 while the I-DBPs concentration plateaued (Figure 2b). The formation of I-THMs is not correlated to
388 the I-DBPs formation and can't be used to assess I-DBPs formation. Therefore, even though
389 increasing HOCl/NH_2Cl concentration does not enhance total I-DBPs formation by halogenation
390 reaction, they play a role in the oxidation/breakdown of halogenated-NOM moieties which may lead
391 to high concentration of I-THMs.

392

393 **3.4 Effect of NOM nature and concentration on iopromide degradation during sequential**
394 **treatment**

395

396 The impact of various NOM concentrations (0 to 4 mgC/L) on IOP degradation (10 µM) and
397 subsequent formation of iodinated organic moieties was studied at an incident photonic flux of 4000
398 $J.m^{-2}$ followed by 5 $mgCl_2/L$ of HOCl or NH_2Cl as disinfectant for 24H (Figure 4a).

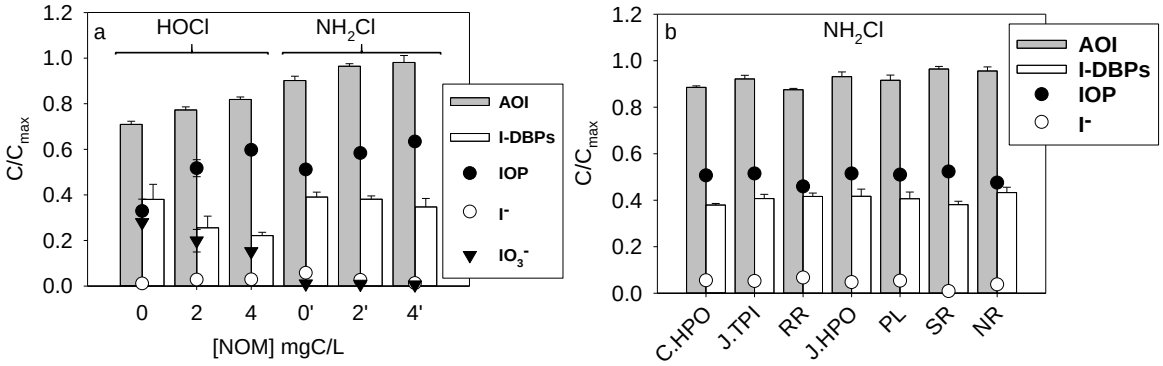

Figure 4: Speciation of iodine after irradiation of iopromide followed by chlorination or chloramination (24H contact time). Impact of (a) NOM concentration, 0-4 mgC/L SR-NOM, (b) NOM type, 2 mgC/L (see Table S1 for NOM characteristics). UV dose 4000 J.m^{-2}, [IOP]$_o$ 10 µM, [HOCl] or [NH_2Cl] 5 mgCl_2/L (24H contact time).

As shown in Figure 4a, IOP degradation decreases with increasing NOM concentration for both oxidants. This is due to UV light absorption by NOM moieties (Frimmel 1998). The exposure of IOP to UV_{254} is reduced, leading to a lower photodegradation of IOP thus a lower formation of photodegradation products containing iodine (accounting for I-DBPs). The total amount of AOI is increasing with increasing NOM concentration for both oxidants but I-DBPs concentration decreases from 38% for 0 mgC/L to 22% for 4 mgC/L with HOCl whereas it is constant (~38%) for all NOM concentration with NH_2Cl. When HOCl is used, the concentration of I-DBPs is decreasing with increasing NOM content because of the smaller degradation of IOP and the concomitant formation of IO_3^-. For the experiments with NH_2Cl, the decrease of IOP degradation due to UV light screening for increasing NOM concentration is compensated by the highest formation of I-DBPs through the reaction of HOI with NOM since more NOM reactive sites are available. This is also evidenced by the decreasing I^- concentration after 24 h with increasing NOM concentration (from 0 to 4 mgC/L). For 4 mgC/L all the I^- is incorporated to organic moieties. It can be concluded that the removal of IOP is higher for waters containing low amount of NOM. However, when NH_2Cl is used after UV treatment, the formation of I-DBPs slightly decreases (or is constant, within the error bars range), while for the experiment with HOCl the formation of I-DBPs is decreasing with increasing NOM concentration.

To better understand the role of NOM in I-DBPs formation in this sequential process, various NOM types were tested under similar experimental conditions. Figure 4b shows the concentration of the various iodinated species for 7 different types of NOM classified by increasing $SUVA_{254}$ values (Table S1). The concentration of IOP after sequential treatment (~ 50%) is similar for all NOM extracts. This shows that, unlike NOM concentration, the higher screening effect induced by high $SUVA_{254}$ NOM is not a critical parameter and does not affect IOP degradation significantly. NOM with higher $SUVA_{254}$

values were also expected to have a higher reactivity toward HOI (Hua and Reckhow, 2007b). However, the AOI concentration as well as the formation of I-DBPs are almost similar for all DOM extracts. The small I-DBPs variations cannot be explained by the different $SUVA_{254}$ of the organic matter extracts. Therefore, the type of NOM does not have a significant impact on the degradation of IOP, the formation of I-DBPs or the iodine speciation. This is in accordance with results obtained for the bromination of different NOM extracts where the same bromine incorporation into NOM was observed across a wide range of $SUVA_{254}$ (Criquet et al., 2015). It was hypothesized that the concentration of NOM moieties reacting by electrophilic aromatic substitution or electron transfer (oxidation) was similar across various NOM sources. Furthermore, HOI reacts with NOM moieties via electrophilic substitution to form AOI or it oxidises NOM moieties resulting in the release of iodide. The released iodide is then reoxidised to HOI by NH_2Cl and has another possibility to form AOI.

3.5 Effect of UV_{254} photolysis followed by chlorination/chloramination on 5 Iodinated Contrast Media in presence of NOM

The effect of UV irradiation at 4000 $J.m^{-2}$ followed by chlorination or chloramination at 5 $mgCl_2/L$ was studied for 5 different iodinated X-ray contrast media at a concentration of 10 µM in presence of 2 mgC/L SR-NOM.

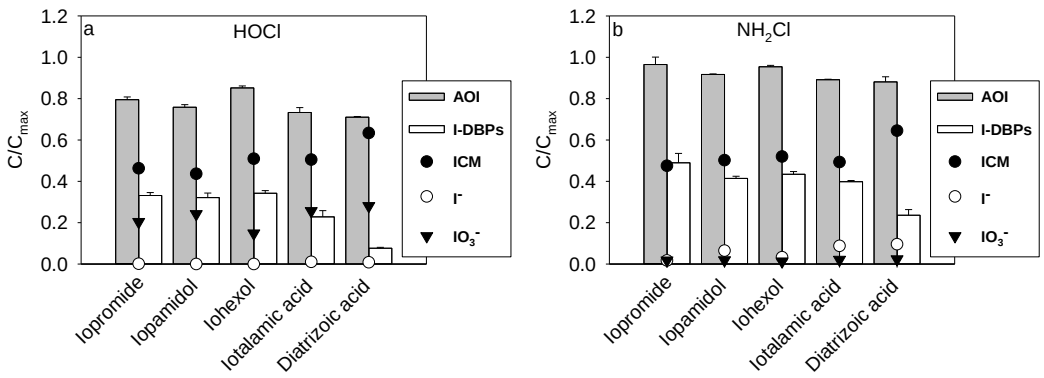

Figure 5: Degradation of 5 ICM by UV irradiation followed by (a) chlorination or (b) chloramination in presence of NOM and speciation of iodine. UV dose 4000 $J.m^{-2}$, $[ICM]_o$ 10 µM, [HOCl] or $[NH_2Cl]$ 5 $mgCl_2/L$ (24H contact time), SR-NOM 2 mgC/L.

In our experimental conditions, the application of HOCl or NH_2Cl after UV treatment to all studied ICM (IOP, iopamidol, iohexol, iotalamic acid and diatrizoic acid) led to the degradation of approximately 50% of the initial iodine concentration with ~5 µM remaining in solution (Figure 5a,b). Diatrizoic acid was less degraded because it has a smaller molar extinction coefficient at 254 nm

(Table 2). This confirms that the degradation mainly occurs through UV photolysis because the ICM are poorly oxidized by NH_2Cl and HOCl, with the exception of iopamidol. The degradation of iopamidol by HOCl and the stability of IOP, iohexol, and diatrizoic acid have already been reported by Wendel et al., (2014). Figure 5a confirms that iodate is formed only with HOCl and that I^- concentrations are negligible in HOCl experiments. The total concentration of AOI is higher for the experiments carried out with NH_2Cl compared to HOCl for all ICM. The same trend is observed for I-DBPs concentration. Since the degradation of all ICM is similar, the evolution of AOI is mostly due to the variation of I-DBPs concentration. Overall, in line with previous results, NH_2Cl promotes the formation of I-DBPs.

3.6 Toxicity testing

Toxicity experiments were performed using AREc32, a bioassay targeting oxidative stress response. Concentration-response curves for experiments with IOP, IOP + UV 4000 $J.m^{-2}$, standard conditions *i.e.* IOP + 2 mgC/L SR-NOM + UV 4000 $J.m^{-2}$ + HOCl or NH_2Cl 5 $mgCl_2/L$ and an extreme scenario with IOP + 4 mgC/L SR-NOM + UV 50000 $J.m^{-2}$ + HOCl or NH_2Cl 5 $mgCl_2/L$ are presented in Figure 6.

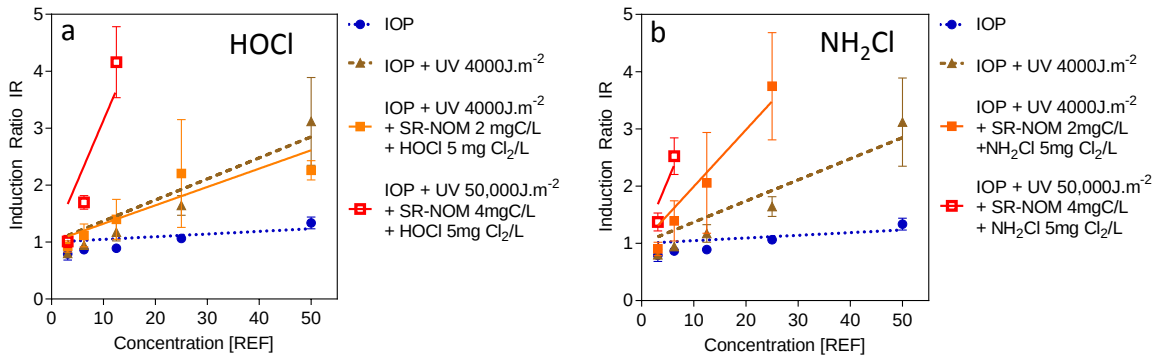

Figure 6: Concentration-effect curves of the linear regression of the AREc32 bioassay (see Figure S8 for the full concentration-effect curves in log scale). Blue dots: Iopromide (IOP); brown triangle: IOP treated with UV 4000 $J.m^{-2}$. Orange filled square: UV 4000 $J.m^{-2}$; red open square: UV 50000 $J.m^{-2}$ for IOP plus SR-NOM 2mgC/L subsequently treated with (a) HOCl or (b) NH_2Cl at 5 $mgCl_2/L$.

Figure 6 showed the induction ratio (IR) of IOP at 10 µM with no induction in oxidative stress at REF tested at 50 (IR < 1.5). This confirmed that IOP itself is not toxic. For the UV experiments, after dosing with 4000 $J.m^{-2}$ the toxic response increased 5 fold from tBHQ-EQ 4.29 µg/L (IOP alone) to 20.60 µg/L (IOP + UV) indicating that the degradation products of IOP (which are I-DBPs) are toxic. This finding underlines that despite the nontoxic effect of the X-ray contrast media, their presence in the environment should be a major concern as the photo-transformation products formed from IOP are toxic. For the HOCl experiment with standard conditions (IOP + 2 mgC/L SR-NOM + UV 4000 $J.m^{-2}$,

478 (Figure 6a, red line)) the toxicity is similar to UV alone (Figure 6a, tBHQ-EQ of 17.97 µg/L). This
479 indicates that the toxicity induced by the formation of I-DBPs from reaction of HOI with NOM is
480 negligible in the case of HOCl and the oxidation of iodide to iodate is efficient in mitigating the
481 oxidative stress response. Conversely, when NH_2Cl was used, *i.e.* no iodate were formed and the
482 formation of I-DBPs was favoured, (Figure 6b, red line), the toxicity increased to a tBHQ-EQ of 55.27
483 µg/L. When the UV dose and the SR-NOM concentration were increased, a further increase in
484 oxidative stress response was observed with a tBHQ-EQ of 119.11 µg/L for the experiment with HOCl
485 (Figure 6a, orange line) and 121.93 µg/L for the experiment with NH_2Cl (Figure 6b, orange line). This
486 was expected since increasing the UV fluence increases the release of iodide and increasing the SR-
487 NOM concentration increases the number of reactive site available for reaction with HOI to form
488 toxic I-DBPs.

489

490 **Conclusion**

491 The impact of the sequential treatment UV_{254} irradiation followed by disinfection with HOCl or NH_2Cl
492 on the degradation of 5 ICM and the formation of toxic I-DBPs was investigated in presence of
493 different concentration and types of NOM. UV_{254} irradiation was proved to be effective in degrading
494 ICM with two quantum yields determined for the first time in this study, diatrizoic acid (0.071
495 mol.Einstein^{-1}), and iotalamic acid (0.038 mol.Einstein^{-1}) and three quantum yields already published
496 in the literature that have been confirmed for IOP (0.039 mol.Einstein^{-1}), iopamidol (0.034
497 mol.Einstein^{-1}) and iohexol (0.041 mol.Einstein^{-1}). The effect of pH on the ICM photodegradation rate
498 was negligible. The photodegradation of the 5 ICM leads to the release of I^- which is increasing with
499 the UV_{254} dose. It was confirmed that HOCl and NH_2Cl were not (or poorly degrading) ICM (iopamidol
500 and iopromide were slightly degraded at high HOCl dose). In presence of NOM, the UV_{254} HOCl/NH_2Cl
501 sequential treatment leads to significant formation of I-DBPs for both oxidant. For high doses of
502 oxidant, HOCl formed less I-DBPs than NH_2Cl since iodate are formed which is non-toxic and the
503 desired sink for iodine in water treatment. Increasing the concentration of NOM reduced the
504 photolysis of IOP through light scavenging. However, it also increases the number of reactive sites
505 available for I-DBPs formation. Increasing NOM concentration decreases the formation of I-DBPs
506 when HOCl was used while it remained constant when NH_2Cl was dosed. 7 different NOM extracts
507 were tested but no appreciable differences were observed in terms of IOP degradation and I-DBPs
508 formation. Therefore, unlike NOM concentration, it can be concluded that the nature of the NOM
509 does not have a significant impact. It was also showed that the 5 ICM behave similarly and it was
510 confirmed that higher concentration of I-DBPs are formed when NH_2Cl is used compared to HOCl.
511 Toxicity tests confirmed the above results with higher toxicity measured for the experiments with

512 NH_2Cl. Interestingly the toxicity observed for the HOCl experiment was similar to the UV_{254} alone
513 experiments, confirming that the formation of IO_3^- inhibits to a great extent the impact of I-DBPs and
514 their associated toxicity. These results showed that ICM are a source of iodine that may lead to the
515 formation of toxic I-DBPs when UV_{254} and final disinfection are applied for drinking water production.
516 This may have important implication in one hand for the treatment of drinking water sources
517 polluted by ICM and in another hand for the UV-implemented tertiary treatment of wastewaters as
518 the phototransformation products of iodinated contrast media could enhance the toxicity of the
519 effluent.

520

521 **Acknowledgments**

522 The authors would like to acknowledge funding and support from Curtin University and University of
523 Lille 1 Sciences and Technologies. Dr. Justine Criquet thanks the French Ministry of Foreign Affairs
524 and International Development (MAE) and the French Ministry of Higher Education and Research
525 (MESR) for the support provided through the program PHC FASIC; Cecilia Falantin thanks the Region
526 Nord-Pas de Calais for the support of her mobility program. We thank S. Canonica for helpful
527 discussions on the calculation of the quantum yields.

528

529 **References**

530 Allard, S., Charrois, J.W.A., Joll, C.A., Heitz, A., 2012. Simultaneous analysis of 10 trihalomethanes at
531 nanogram per liter levels in water using solid-phase microextraction and gas chromatography mass-
532 spectrometry. J. Chromatog. A. 1238, 15-21.
533
534 Allard, S., Tan, J., Joll, C.A., von Gunten, U., 2015. Mechanistic Study on the Formation of Cl-/Br-/I-
535 Trihalomethanes during Chlorination/Chloramination Combined with a Theoretical Cytotoxicity
536 Evaluation. Environ. Sci. Technol. 49 (18), 11105-11114.
537
538 Allard, S., von Gunten, U., Sahli, E., Nicolau, R., Gallard, H., 2009. Oxidation of iodide and iodine on
539 birnessite (δ-MnO_2) in the pH range 4-8. Water Res. 43 (14), 3417-3426.
540
541 APHA, A., WPCF, 1998. Standard Methods for the Examination of Water and Wastewater,
542 Washington.
543
544 Bichsel, Y., von Gunten, U., 1999. Oxidation of Iodide and Hypoiodous Acid in the Disinfection of
545 Natural Waters Environ. Sci. Technol. 33 (22), 4040-4045.
546
547 Bichsel, Y., von Gunten, U., 2000a. Formation of Iodo-Trihalomethanes during Disinfection and
548 Oxidation of Iodide-Containing Waters. Environ. Sci. Technol. 34 (13), 2784-2791.
549
550 Bichsel, Y., von Gunten, U., 2000b. Hypoiodous acid: Kinetics of the buffer-catalyzed
551 disproportionation. Water Res. 34 (12), 3197-3203.

Burgi, H., Schaffner, T., Seiler, J.P., 2001. The toxicology of iodate: A review of the literature. Thyroid 11 (5), 449-456.

Busetti, F., Linge, K.L., Rodriguez, C., Heitz, A., 2010. Occurrence of iodinated X-ray contrast media in indirect potable reuse systems. J. Environ. Sci. Heal. A. 45 (5), 542-548.

Canonica, S., Meunier, L., von Gunten, U., 2008. Phototransformation of selected pharmaceuticals during UV treatment of drinking water. Water Res. 42 (1-2), 121-128.

Christiansen, C., 2005. X-ray contrast media - an overview. Toxicology 209 (2), 185-187.

Criquet, J., Allard, S., Salhi, E., Joll, C.A., Heitz, A., von Gunten, U., 2012. Iodate and iodo-trihalomethane formation during chlorination of iodide-containing waters: Role of bromide. Environ. Sci. Technol. 46 (13), 7350-7357.

Criquet, J., Rodriguez, E.M., Allard, S., Wellauer, S., Salhi, E., Joll, C.A., von Gunten, U., 2015. Reaction of bromine and chlorine with phenolic compounds and natural organic matter extracts - Electrophilic aromatic substitution and oxidation. Water Res. 85, 476-486.

Doll, T.E., Frimmel, F.H., 2003. Fate of pharmaceuticals - Photodegradation by simulated solar UV-light. Chemosphere 52 (10), 1757-1769.

Drewes, J.E., Fox, P., Jekel, M., 2001. Occurrence of iodinated X-ray contrast media in domestic effluents and their fate during indirect potable reuse. J. Environ. Sci. Heal. A. 36 (9), 1633-1645.

Duirk, S.E., Lindell, C., Cornelison, C.C., Kormos, J., Ternes, T.A., Attene-Ramos, M., Osiol, J., Wagner, E.D., Plewa, M.J., Richardson, S.D., 2011. Formation of toxic iodinated disinfection by-products from compounds used in medical imaging. Environ. Sci. Technol. 45 (16), 6845-6854.

Escher, B.I., Van Daele, C., Dutt, M., Tang, J.Y.M., Altenburger, R., 2013. Most oxidative stress response in water samples comes from unknown chemicals: The need for effect-based water quality trigger values. Environ. Sci. Technol. 47 (13), 7002-7011.

Frimmel, F.H., 1998. Impact of light on the properties of aquatic natural organic matter. Environ. Int. 24 (5–6), 559-571.

Gartiser, S., Brinker, L., Erbe, T., Kümmerer, K., Willmund, R., 1996. Contamination of hospital wastewater with hazardous compounds as defined by § 7a WHG. Acta Hydroch. Hydrob.24 (2), 90-97.

Hua, G., Reckhow, D.A., 2007a. Comparison of disinfection byproduct formation from chlorine and alternative disinfectants. Water Res. 41 (8), 1667-1678.

Hua, G., Reckhow, D.A., 2007b. Characterization of disinfection byproduct precursors based on hydrophobicity and molecular size. Environ. Sci. Technol. 41 (9), 3309-3315.

Jones, D.B., Saglam, A., Triger, A., Song, H., Karanfil, T., 2011. I-THM formation and speciation: Preformed monochloramine versus prechlorination followed by ammonia addition. Environ. Sci. Technol. 45 (24), 10429-10437.

Jortner, J., Levine, R., Ottolenghi, M., Stein, G., 1961. The photochemistry of the iodide ion in aqueous solution. J. Phys. Chem-US. 65 (7), 1232-1238.

Katsoyiannis, I.A., Canonica, S., von Gunten, U., 2011. Efficiency and energy requirements for the transformation of organic micropollutants by ozone, O_3/H_2O_2 and UV/H_2O_2. Water Res. 45 (13), 3811-3822.

Kristiana, I., Gallard, H., Joll, C., Croué, J.P., 2009. The formation of halogen-specific TOX from chlorination and chloramination of natural organic matter isolates. Water Res. 43 (17), 4177-4186.

Lee, Y., Yoon, J., von Gunten, U., 2005. Kinetics of the oxidation of phenols and phenolic endocrine disruptors during water treatment with ferrate (Fe(VI)). Environ. Sci. Technol. 39 (22), 8978-8984.

Leenheer, J.A., Croue, J.P., 2003. Characterizing aquatic dissolved organic matter. Environ. Sci. Technol. 37 (1), 18A-26A.

Nicole, I., Delaat, J., Dore, M., Duguet, J.P., Bonnel, C., 1990. Use of Uv-Radiation in Water-Treatment - Measurement of Photonic Flux by Hydrogen-Peroxide Actinometry. Water Res. 24 (2), 157-168.

Pereira, V.J., Weinberg, H.S., Linden, K.G., Singer, P.C., 2007a. UV degradation kinetics and modeling of pharmaceutical compounds in laboratory grade and surface water via direct and indirect photolysis at 254 nm. Environ. Sci. Technol. 41 (5), 1682-1688.

Pereira, V.J., Linden, K.G., Weinberg, H.S., 2007b. Evaluation of UV irradiation for photolytic and oxidative degradation of pharmaceutical compounds in water. Water Res. 41 (19), 4413-4423.

Pérez, S., Barceló, D., 2007. Fate and occurrence of X-ray contrast media in the environment. Anal. Bioanal. Chem. 387 (4), 1235-1246.

Pérez, S., Eichhorn, P., Ceballos, V., Barceló, D., 2009. Elucidation of phototransformation reactions of the X-ray contrast medium iopromide under simulated solar radiation using UPLC-ESI-QqTOF-MS. J. Mass Spectrom. 44 (9), 1308-1317.

Plewa, M.J., Muellner, M.G., Richardson, S.D., Fasano, F., Buettner, K.M., Woo, Y.T., McKague, A.B., Wagner, E.D., 2008. Occurrence, synthesis, and mammalian cell cytotoxicity and genotoxicity of haloacetamides: An emerging class of nitrogenous drinking water disinfection byproducts. Environ. Sci. Technol. 42 (3), 955-961.

Plewa, M.J., Wagner, E.D., Richardson, S.D., Thruston Jr, A.D., Woo, Y.T., McKague, A.B., 2004. Chemical and biological characterization of newly discovered iodoacid drinking water disinfection byproducts. Environ. Sci. Technol. 38 (18), 4713.

Putschew, A., Schittko, S., Jekel, M., 2001. Quantification of triiodinated benzene derivatives and X-ray contrast media in water samples by liquid chromatography-electrospray tandem mass spectrometry. J. Chromatog. A. 930 (1-2), 127-134.

Putschew, A., Wischnack, S., Jekel, M., 2000. Occurrence of triiodinated X-ray contrast agents in the aquatic environment. Sci. Total Environ.255 (1-3), 129-134.

Richardson, S.D., Fasano, F., Ellington, J.J., Crumley, F.G., Buettner, K.M., Evans, J.J., Blount, B.C., Silva, L.K., Waite, T.J., Luther, G.W., McKague, A.B., Miltner, R.J., Wagner, E.D., Plewa, M.J., 2008.

Occurrence and mammalian cell toxicity of iodinated disinfection byproducts in drinking water. Environ. Sci. Technol. 42 (22), 8330.

Salhi, E., von Gunten, U., 1999. Simultaneous determination of bromide, bromate and nitrite in low µg l^{-1} levels by ion chromatography without sample pretreatment. Water Res. 33 (15), 3239.

Sauer Jr, M.C., Crowell, R.A., Shkrob, I.A., 2004. Electron photodetachment from aqueous anions. 1. Quantum yields for generation of hydrated electron by 193 and 248 nm laser photoexcitation of miscellaneous inorganic anions. J. Phys. Chem. A. A 108 (25), 5490-5502.

Tang, J.Y.M., McCarty, S., Glenn, E., Neale, P.A., Warne, M.S.J., Escher, B.I., 2013. Mixture effects of organic micropollutants present in water: Towards the development of effect-based water quality trigger values for baseline toxicity. Water Res. 47 (10), 3300-3314.

Ternes, T.A., Hirsch, R., 2000. Occurrence and behavior of X-ray contrast media in sewage facilities and the aquatic environment. Environ. Sci. Technol. 34 (13), 2741-2748.

Tian, F.X., Xu, B., Lin, Y.L., Hu, C.Y., Zhang, T.Y., Gao, N.Y., 2014. Photodegradation kinetics of iopamidol by UV irradiation and enhanced formation of iodinated disinfection by-products in sequential oxidation processes. Water Res. 58, 198-208.

Wendel, F.M., Lütke Eversloh, C., Machek, E.J., Duirk, S.E., Plewa, M.J., Richardson, S.D., Ternes, T.A., 2014. Transformation of iopamidol during chlorination. Environ. Sci. Technol. 48 (21), 12689-12697.

Wendel, F.M., Ternes, T.A., Richardson, S.D., Duirk, S.E., Pals, J.A., Wagner, E.D., Plewa, M.J., 2016. Comparative Toxicity of High-Molecular Weight Iopamidol Disinfection Byproducts. Environ. Sci. Technol. Letters. 3 (3), 81-84.

Wolfe, R.L., 1990. Ultraviolet disinfection of potable water: Current technology and research needs. Environ. Sci. Technol. 24 (6), 768-773.

Wols, B.A., Hofman-Caris, C.H.M., 2012. Review of photochemical reaction constants of organic micropollutants required for UV advanced oxidation processes in water. Water Res. 46 (9), 2815-2827.

Ye, T., Xu, B., Wang, Z., Zhang, T.Y., Hu, C.Y., Lin, L., Xia, S.J., Gao, N.Y., 2014. Comparison of iodinated trihalomethanes formation during aqueous chlor(am)ination of different iodinated X-ray contrast media compounds in the presence of natural organic matter. Water Res. 66, 390-398.